Construction and Building Materials 230 (2020) 116873

Contents lists available at ScienceDirect

Construction and Building Materials

journal homepage: www.elsevier.com/locate/conbuildmat

Effects of stirrups in spliced region on the bond strength of corroded splices in reinforced concrete (RC) beams

Yaser Moodi, Mohammad Reza Sohrabi *, Seyed Roohollah Mousavi

Civil Engineering Department, University of Sistan and Baluchestan, Zahedan, Iran

HIGHLIGHTS

- Effects of confinement on the bond strength of corroded RC beams are investigated.
- An increase in stirrups increase the bond strength of corroded RC beams.
- Ductility and energy dissipation potential of beams are affected by stirrups.

ARTICLE INFO

Article history:
Received 24 February 2019
Received in revised form 30 June 2019
Accepted 1 September 2019

Keywords:
Corrosion
Beam
Lap spliced
Bond
Reinforced concrete

ABSTRACT

This study has addressed effects of stirrups-caused confinement on the concrete-bar bond strength of lap-spliced RC beams which have been corroded. Twenty of such beams with different stirrup spacing in the spliced region were subjected to corrosion, and the percentages of corrosion of the lap-spliced tensile bars were considered as the variable of this study; these beams were tested under four-point bending test. Tests results have shown that the increased stirrups in the spliced region increased the bond strength, ductility, and energy dissipation potential. Stirrups were more effective in high corrosion; at 25% corrosion.

1. Introduction

The steel bar corrosion is the main failure cause of RC structures. When rebars get corroded, they expand volumetrically (because of the composition of the corroded materials) and become several times the ordinary rebars in volume. This corrosion-caused volume increase results in tension in the concrete around rebars [1–5] which, in turn, causes the cracking and splitting of the concrete cover. In the specific type of corrosion caused by chloride type, the cracking will cause the chlorine ion to reach the rebar surface more quickly causing the corrosion to continue faster.

In General, the force created on the rebar has horizontal and vertical components (with or without corrosion); the former is the bond force and the latter splits up the concrete. The concrete-rebar bond strength depends on: (1) chemical adhesion, (2) friction, and (3) mechanical interaction. The last item depends on the rebar confinement created by the concrete and stirrups and has the greatest effect on the bond in deformed rebars [6].

Tests to determine the bond strength can be divided into three general categories [7]:

1. Pullout and Beam-end Tests: where the concrete and rebars lie under compression and tension, respectively; hence, the results of these tests will differ from those of real structures where the concrete and rebars lie under compression or tension simultaneously.
2. Tension Stiffening Test: where the concrete and rebars lie simultaneously under tension (this test condition is more similar to that of the real structure).
3. Actual Beam Test: where a real structure is tested under four-point bending with both lap-spliced and non-spliced beams.

Corrosion effects on steel bars are quite serious; the bar cross-section and concrete-bar bond strength will both be reduced. Zhao et al. [8] have shown that when corrosion reaches 14% (i.e., rebar cross-section is reduced by 14%), the bond strength will be reduced by more than 80–90%, meaning that the corrosion effect on

* Corresponding author.
E-mail addresses: sohrabi@hamoon.usb.ac.ir (M.R. Sohrabi), s.r.mousavi@eng.usb.ac.ir (S.R. Mousavi).

https://doi.org/10.1016/j.conbuildmat.2019.116873
0950-0618/

reducing the bond strength is greater than that on the cross-section. Earlier studies have shown that the rebar corrosion has a significant effect on the final concrete-bar bond strength; when corrosion is low, the bond strength may increase, but severe rebar corrosion will significantly reduce the concrete-bar bond strength [9–13].

Studies on the corrosion effects on the bond strength through the mentioned tests are numerous; Al-Sulaymani et al. [9], Law et al. [11], Tondolo [12], Zhang et al. [13], Lee et al. [1], Yalciner et al. [14], and Zhang et al. [15] are among those who have used the Pullout Test for this purpose. In a study on the effects of the transverse reinforcement on the bond strength, Lee et al. [1] have shown that in the stress-slip curve, the residual stress after the maximum strength for specimens with transverse reinforcement is larger than the residual stress for specimens without transverse reinforcement. A study on the effects of corrosion on the bond strength has shown that corrosion affects smooth bars more than deformed bars [16]. The magnitude of the reduction in residual bond strength for different corrosion percent has been reported in fib Model Code 2010 [17], which confirms the finding of Ma et al. [16] research. Effect of corrosion on bond strength depend on the degree of confinement provided by secondary reinforcement [17]. Law et al. [11] have investigated the confinement effects through the beam-end test and have shown that confinement affects cracking and increase bond strength in equal-width cracks. They have also shown that when the concrete cover increases, the stirrup effect decreases. Zhang et al. [15] have studied corrosion effects on the bond strength with different strain rates and have shown that an increase in the concrete cover will cause a limited increase in the bond strength in specimens without stirrups while the increase is significant in specimens with stirrups [18,19]. In a push-out test conducted to show the corrosion effects on the bond strength, Sanz et al. [20] have shown that corrosion will affect the residual stress after the peak load.

Researchers who have studied the corrosion effects on the bond strength through the Tension Stiffening Test include Shayanfar and Ghalenovi [10], Amleh and Mirza [21], Dai et al. [22], Aryanto and Shinohara [23], and Kim et al. [24]. Dai et al. [22] have investigated the effects of stirrups on the bond strength of the corroded bars. Studies on the corrosion effects on the bond strength of actual beams are not many [6, 9, and 25–27].

Using non-spliced beams to study the corrosion effects on the bond strength, Zhao et al. [8] have shown that the strength of such beams is greater than that found in the Pullout test due mainly to the supports' lateral pressure on the longitudinal bars. Al-Hammoud et al. [26] have examined the support-/stirrup-caused confinement effects on the concrete-bar bond strength in non-spliced beams and have shown that a decrease in the stirrup spacing will increase the bond strength and change the specimen's failure mode; when stirrups are spaced apart, an increased development length will have no effects on the bond strength. In a study on the stirrup effects on the bond strength of non-spliced beams with corroded longitudinal rebars, Lin and Zhao [6] have shown that stirrups have significant effects on the crack propagation. Reduced stirrup spacing will mitigate(slow down) the propagation of the corrosion-caused cracks, but when stirrups are spaced apart, the bond strength reduction is more severe. Studies on the corrosion effects on the bond strength of lap-spliced beams are few; here, since the splice is in the beam mid-span, the support-caused confinement effect is eliminated. In a study on the corrosion effects on the bond strength, Shihata [27] has shown, using the lap-spliced beam test, that both the rebar diameter and concrete cover affect the bond strength of the corroded bars. The variables were the concrete cover-to-splice bar diameter ratio and the percentage of corrosion, and the stirrup-caused confinement was not considered in the spliced region.

The current study has addressed the confinement (with stirrups) and high corrosion effects (25%) on the bond strength of the lap-spliced corroded RC beams considering percentage of corrosion and stirrup spacing in the spliced region as variables (earlier studies have dealt less with this issue). Results have shown that using more stirrups in the splice region will increase the beams' bond strength and efficiency. These stirrups have greater effects on the bond strength, ductility, and energy dissipation potential in high corrosion.

2. Experimental program

2.1. Test specimens

Twenty lap-spliced RC beams 150 × 200 mm in cross section and 2000 mm in length were examined under four-point bending test. Tensile bars, spliced at the mid-span, were two 12 mm-diameter steel bars, while the compressive ones were two continuous 8 mm-diameter bars. To let the bond failure to prevail in beams, the splice length (Ld) was taken to be 20 cm (insufficient overlapping, according to the equation in the ACI 318M-11 [28] without considering a safety factor), and to prevent shear failure, 8 mm-diameter stirrups were spaced 80 mm apart in the region outside the splice. Fig. 1 shows the specimens' dimensions, supports' distances, and the net bending length. Dimensions are in millimeter in Fig. 1.

Variables of this study are the number of stirrups (0, 1, 2 and 3) and percentage of corrosion of tensile bars (0, 2, 5, 10, and 25%) in the splice region (i.e. the stirrup spacing is 200, 100, 66, and 50 mm). As mentioned before, high corrosion rates have not been addressed sufficiently in previous studies; this research has considered it to be up to 25% which is sufficiently high. The specimen naming is according to G1SbCi where b is the number of stirrups in the splice region and i is the percentage of corrosion of the tensile bar.

2.2. Material specifications

The concrete used in this study was in-situ, all aggregates were sieved, similar gradation was used for all specimens, and the largest aggregate size was 19 mm. The mix design for concrete strength was selected to be 25 MPa and is shown in Table 1. To determine the concrete compressive strength, use was made of 300 × 150 cylindrical specimens for which the average compressive strength was found to be 24.5 MPa. For compressive bars/stirrups and tensile bars, use was made of 8 and 12 mm-diameter deformed bars (types AII and AIII, respectively). The mechanical specifications of the bars used in this study were found based on DIN EN 10002 [29] tensile test; the yield strengths of the 8 and 12 mm bars were 376 and 451 MPa, respectively. To avoid stirrups to corrode, they were covered by epoxy resin, and to prevent the current to pass through the interface between the stirrups and longitudinal bars, stirrups bars were covered with electric insulating glue. Fig. 2 shows these stirrups.

2.3. Accelerated corrosion

Using natural corrosion (occurred in the long run) is preferred if the corrosion process is to be checked in the concrete-bar bond region. To speed up this process, researchers make extensive use of the accelerated corrosion process wherein the specimen is corroded using a solution of 5% NaCl. Regarding the current study, the solution was poured in the lavers provided in the mid-span of the beam (Fig. 3). Dimensions of the container were 200 × 150 × 100 mm.

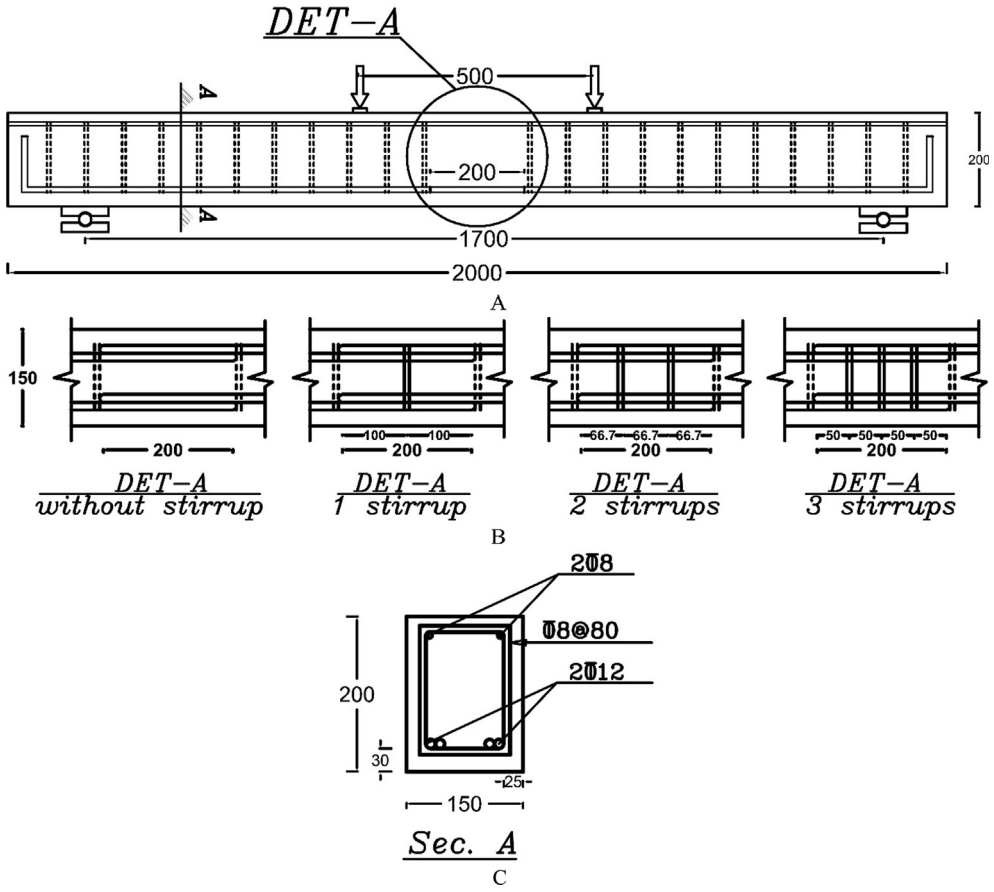

Fig. 1. Specimen details: A. Casting and testing position, B. The splice region and C. Cross section.

Table 1
Mix design of concrete.

W/C	Unit weight (kg/m^3)			
	Water	Cement	Fine aggregate	Coarse aggregate
0.59	220	372.88	866	869

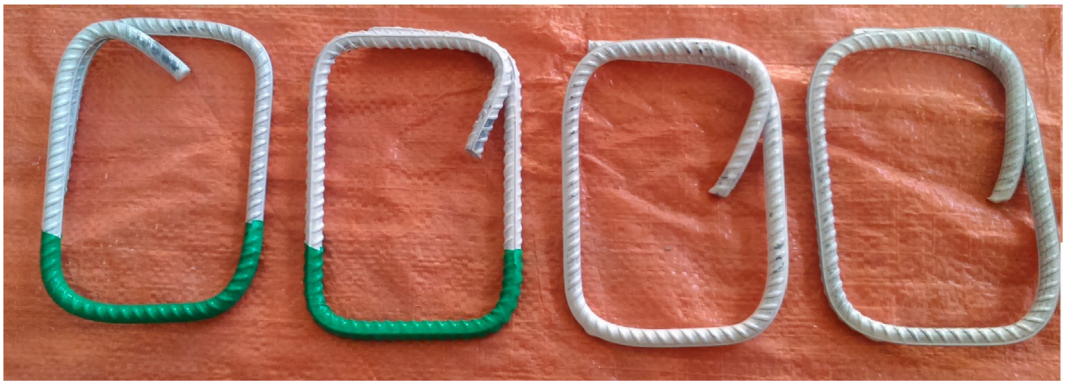

Fig. 2. Painted and insulated stirrups.

For tensile bars in the splice region (200 mm in the beam mid-span), corrosion levels of 2, 5, 10, and 25% were selected, and to estimate the corrosion current duration for these levels, use was made of the Faraday Law:

$$T = \frac{2Fm_t}{55.847I} \quad (1)$$

where I (Ampere) is the impressing current, T is the impressing current duration, F is the Faraday constant (96425 c/mol), and m_t is the loss of the iron mass.

El Maaddawy and Soudki [30] have shown that an increase in the corrosion current (above 200 μA/cm^2), will significantly increase the strain response and the crack width due to the rebar corrosion. Therefore, when the density of the applied current is

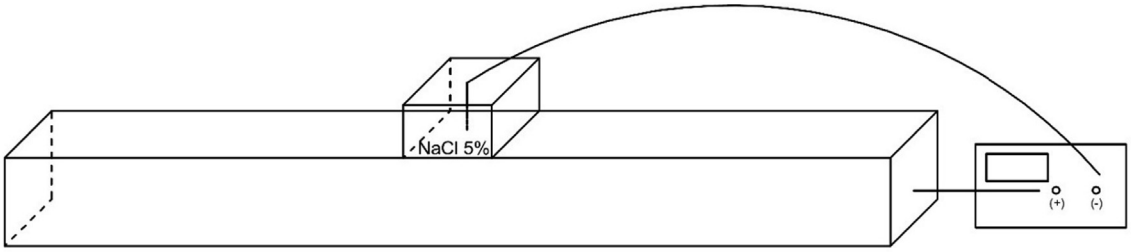

Fig. 3. Electrical connection of the system.

Table 2
Actual corrosion (%).

Specimen	G1S0C2	G1S0C5	G1S0C10	G1S0C25	G1S1C2	G1S1C5	G1S1C10	G1S1C25
Actual corrosion	1.4	4.98	9.79	20.43	1.97	5.76	11.54	20.28
Specimen	G1S2C2	G1S2C5	G1S2C10	G1S2C25	G1S3C2	G1S3C5	G1S3C10	G1S3C25
Actual corrosion	2.69	3.91	9.41	17.44	3.1	5.28	8.81	23.67

high, the corrosion products will have different morphologies from those of the natural ones. Saifullah and Clark [31] believe that corrosion values greater than 250 ($\mu A/cm^2$) can have more negative effects on the structure than the natural corrosion. In the current study use was made of the accelerated corrosion process with a constant current density of 190 ($\mu A/cm^2$); the corrosion current was applied to the splice's four tensile bars (acting as anodes) and the stainless steel inside the NaCl solution laver (acting as cathodes). Considering the current density of 190 ($\mu A/cm^2$), the length and diameter of bars in lap splice zone, the duration of the corrosion process are calculated 10, 25, 100 and 150 days for corrosion levels of 2, 5, 10, and 25%, respectively.

To measure the corrosion rate after loading the beams, the corroded tensile bars were removed from the beams, cleaned by acid washing, and weighed according to G1-03 Code [32]; percentage of corrosion was calculated as follows:

$$\eta = \frac{\bar{m}_0 l - m_c}{\bar{m}_0 l} \tag{2}$$

where $\bar{m}_0$ is the weight per unit length of the un-corroded bar, l is the length of the corroded bar, and m_c is the weight of the corroded bar; the measured corrosion values are given in Table 2.

2.4. Loading procedure, loading pattern, and equipment

The specimens, with span lengths of 1700 mm on simple supports, were examined using the four-point bending test. The loading was applied first through the jack to a rigid steel beam and then to the RC beam in the form of two concentrated forces 500 mm apart. The applied force was measured by a load cell located between the jack and the load distributor rigid beam, the deflection was measured by two LVDT measuring rulers, and the general information (applied load and the beam mid-span displacement) was recorded by a data logger.

3. Results and discussions

3.1. Corrosion and corrosion-caused cracks

When current was being applied on the specimens, effects of the corrosion product formation as well as the corrosion-caused cracks were visible on the surfaces of all the corroded specimens. Corrosion products had reached the concrete surface through these cracks. The crack initiation time was approximately 10 days for all specimens and they were created along the longitudinal bars on the beam's side surface. Fig. 4 shows an example of the cracks formed on the concrete surface at different corrosion levels. After beams were loaded, the tensile bars were brought out of the concrete, cleaned, and used to calculate the actual corrosion according to Code G1-03 [32]; Table 2 shows these corrosion percentages for each specimen. Results show that actual corrosion percentages are less than the theoretical ones and the stirrup spacing does not significantly affect the length of the corrosion-caused cracks. Fig. 4 shows the corroded bars after cleaning at different corrosion levels.

3.2. Failure modes and loading-caused crack patterns

Since the splice length has been selected to be short in all specimens, the failure mode in all of them is of the bond failure type. Figs. 5–8 shows the specimens' cracking pattern where those caused by corrosion are dotted line, and those from loading are of other colors.

The first set of bending cracks in non-corroded specimens occurred at a load of about 10 kN, in the transverse direction of the beams, while in the corroded ones they appeared below that load. In all corroded specimens, cracks along the splice occurred at loads smaller than those of the corresponding non-corroded ones; this has been the case in specimens with fewer stirrups. In most specimens with 5% (or more) corrosion, new cracks did not appear along the splice; only the existing corrosion-caused cracks continued.

As shown in Figs. 5–8, the number of loading-caused cracks decreases with an increase in corrosion while it increases with an increase in the number of stirrups in the splice region. As mentioned before, in specimens with 2 and 3 stirrups in the splice region, the loading-caused cracks along the splice are less visible in the bottom surface, and in the corresponding corroded specimens, the loading-caused splice cracks are fewer and shorter in length. This may be due to the simultaneous presence of the corrosion-caused cracks and increased number of stirrups in the splice region. In addition to the above reason, fewer cracks can be also due to lower bond caused by corrosion.

3.3. Load-displacement diagram, maximum strength, and initial stiffness

Fig. 9 shows, based on the data logger results, the mid-span displacement-load diagram for specimens with equal stirrups but different corrosion percentages, and Table 3 shows the maximum

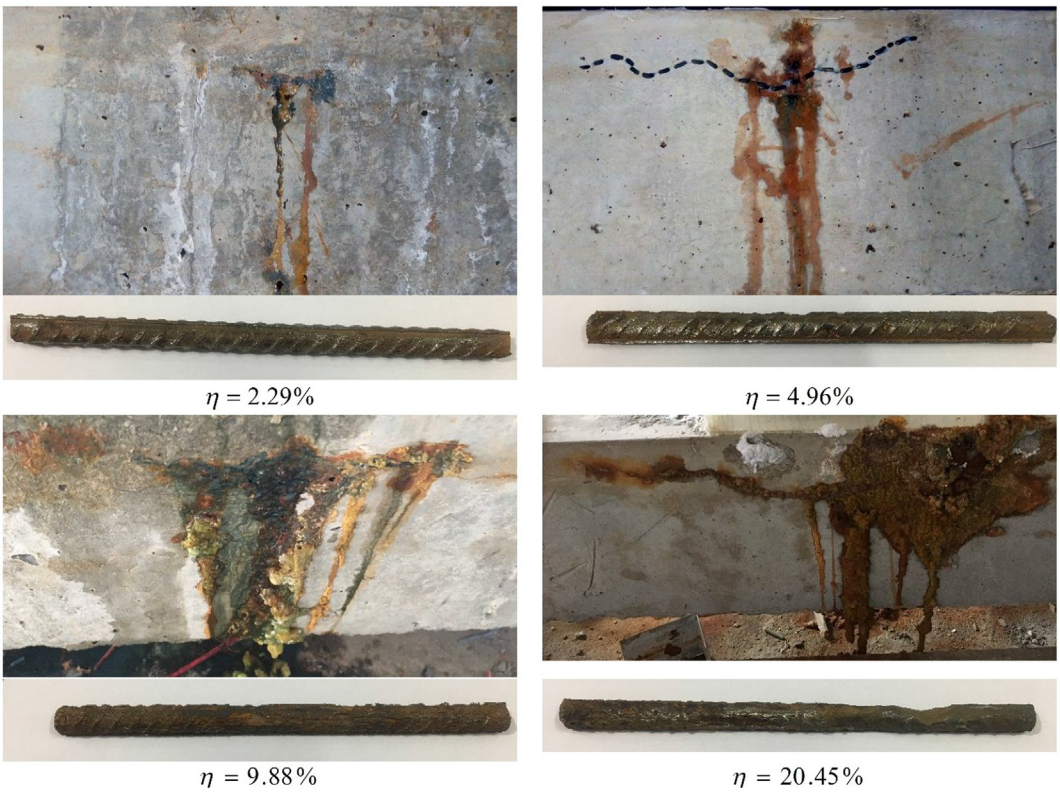

Fig. 4. The corrosion-caused cracks and corroded bars after cleaning.

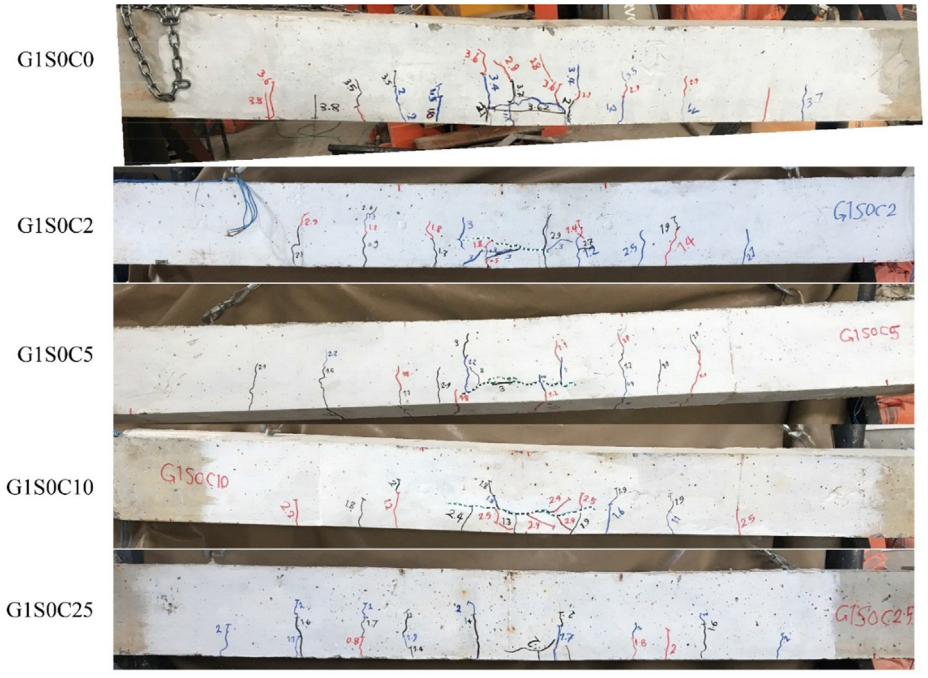

Fig. 5. The cracking pattern of specimens without stirrup.

load capacity of the beams. From the tests, it seems that; when the splice region lacks stirrups, corrosion always reduces the bond strength, but with stirrups, low corrosion (2%) increases the beam strength; in beams with 0, 1, 2 and 3 stirrups in the splice region, 2% corrosion reduces the bond strength by 10%, reduces it slightly, increases it by 4%, and increases it by 8%, respectively.

To better understand the effects of the stirrup spacing on the bond strength of spliced beams, Fig. 10 shows the relative bond strength (R_τ) versus percentage of corrosion; $R_\tau$is defined as the ratio of the corroded specimen bond strength ($\tau_u(c)$) to the bond strength of its corresponding non-corroded specimen ($\tau_u(0)$) as follows:

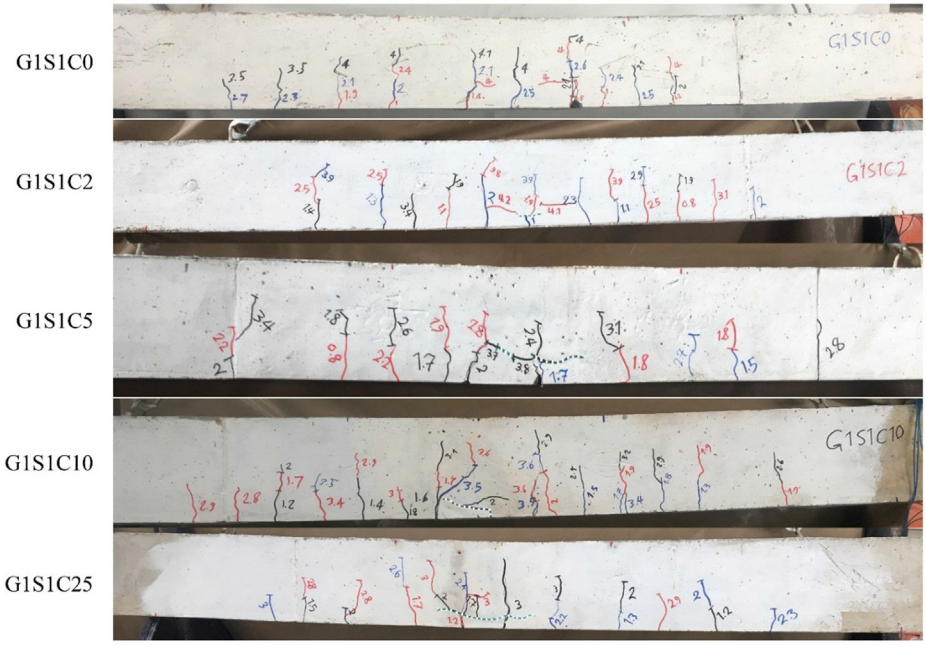

Fig. 6. The cracking pattern of specimens 1 stirrup.

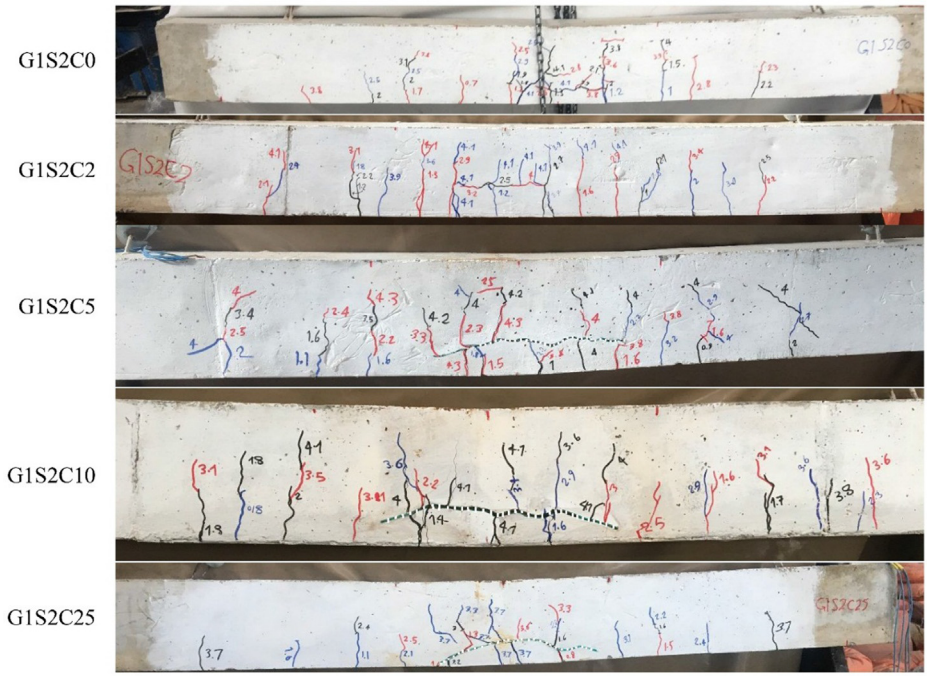

Fig. 7. The cracking pattern of specimens 2 stirrups.

$$R_\tau = \frac{\tau_u(c)}{\tau_u(0)} \tag{3}$$

Results show that increased stirrups in the splice region affect the bond strength of the corroded bars positively, i.e. the gradient of the descending branch of the curve in Fig. 10, found through the best fit of the linear equation, is reduced. For beams with 0, 1, 2, and 3 stirrups in the splice region, this gradient is −0.0198, −0.0154, −0.0136, and −0.0123, respectively. This shows that stirrups with larger spacing affect the bond strength of the lap-spliced corroded beams more; 1 stirrup reduces this gradient by 22% (compared to non-stirrup), but 3 stirrups reduce it by 10% (compared to 2 stirrups).

To have a better understanding of the stirrup effect on the bond strength increase, the percentage of increased load due to the increase in stirrups, compared to the non-stirrup case, is given in Table 4. The data show that the bond strength increase is higher in specimens with corroded tensile bars. The highest increase is related to 25% corrosion. Under this circumstance, the percentage of bond strength increase for beams with 1, 2, and 3 stirrups in the splice region is 4.24, 5.97, and 4.81 times that in the non-corroded case, respectively.

High corrosion cases have not been sufficiently dealt with in earlier studies and some have shown that stirrups have no effects on the bond strength of the corroded bars; however, the results of

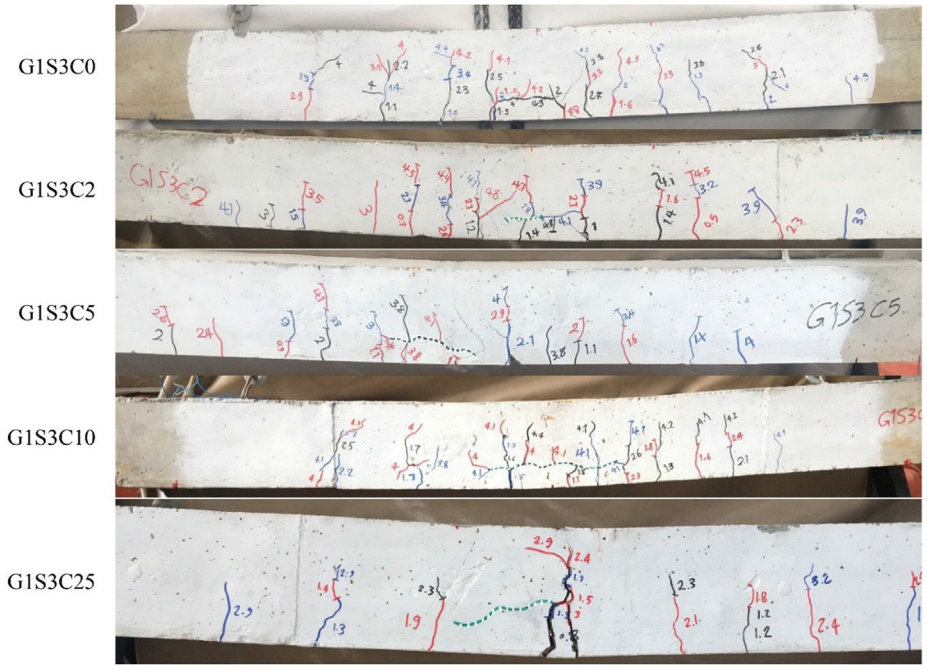

Fig. 8. The cracking pattern of specimens 3 stirrups.

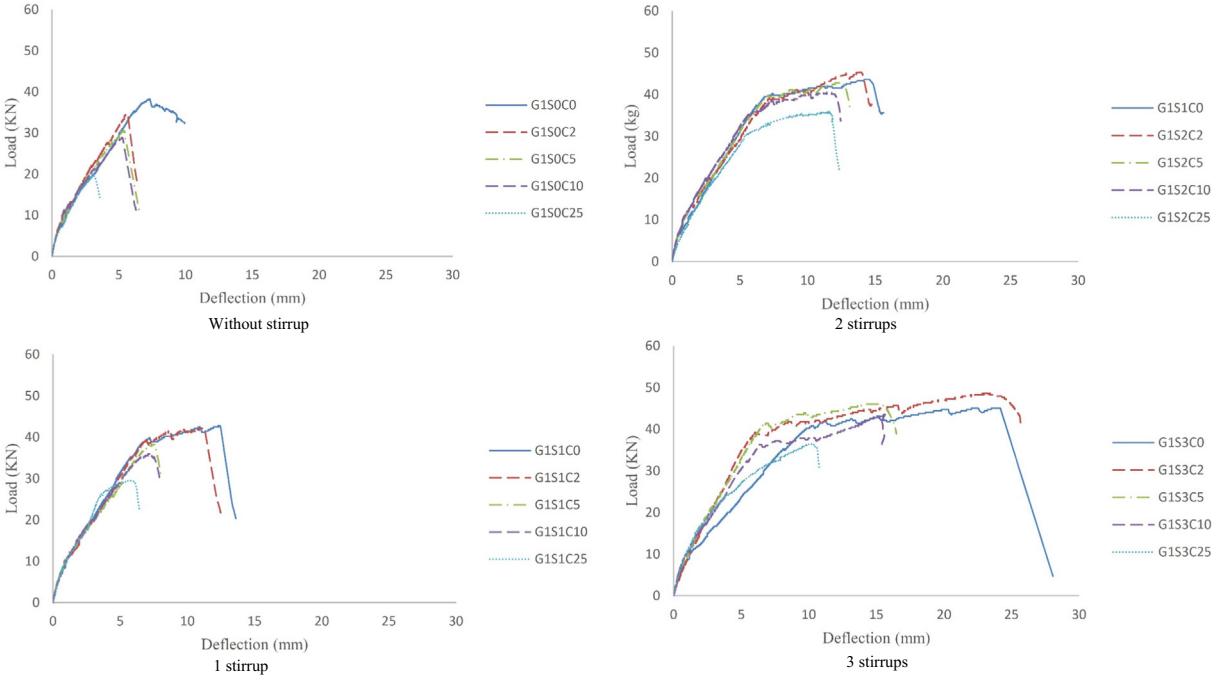

Fig. 9. Displacement-load diagram.

the current study show that stirrups have higher effects in high corrosion cases.

The initial stiffness (K) is defined as the gradient of the load-displacement curve in the linear region. The initial stiffness has been calculated for all the specimens, by using Microsoft Excel, and are shown in Table 3; as shown, increase in corrosion always reduces the initial stiffness. In less-corroded specimens, the initial stiffness is always reduced compared to non-corroded ones, but regarding the bond strength, low corrosion increases it.

3.4. Ductility and energy dissipation potential

To calculate ductility, use has been made of the ductility index proposed by Cohn and Bartlett [33] who defined it as the ratio of the displacement corresponding to 85% of the maximum force (on the descending branch of the load-displacement curve) to the displacement corresponding to the maximum force in the elastic behavior region (Fig. 11).

Ductility index (μ) was calculated for all specimens (Table 3); as shown, increased corrosion reduces the ductility index. Results

Table 3
Summary of specimen results.

	η (%)	P(kN)	K(kN/mm)	μ	E(kN.mm)
G1S0C0	0.00	38.24	12.82	3.23	257.47
G1S0C2	2.29	34.63	12.51	2.19	133.73
G1S0C5	4.69	30.65	11.82	2.41	124.49
G1S0C10	9.88	28.89	10.69	2.19	113.40
G1S0C25	20.43	19.66	8.03	1.55	45.82
G1S1C0	0.00	42.77	11.15	3.41	415.57
G1S1C2	2.29	42.12	10.55	3.00	364.43
G1S1C5	4.69	38.37	9.41	2.04	190.21
G1S1C10	9.88	35.97	8.36	1.94	185.27
G1S1C25	20.43	29.53	7.95	1.84	131.27
G1S2C0	0.00	43.62	10.32	3.72	499.95
G1S2C2	2.29	45.34	10.84	3.60	471.65
G1S2C5	4.69	43.05	9.40	3.20	412.39
G1S2C10	9.88	40.55	9.15	2.96	377.96
G1S2C25	20.43	35.91	7.28	2.50	317.49
G1S3C0	0.00	45.04	9.68	5.39	939.69
G1S3C2	2.29	48.61	8.04	4.32	1005.14
G1S3C5	4.69	46.02	8.55	3.20	584.64
G1S3C10	9.88	43.48	7.81	2.95	486.70
G1S3C25	20.43	36.47	7.53	2.40	276.09

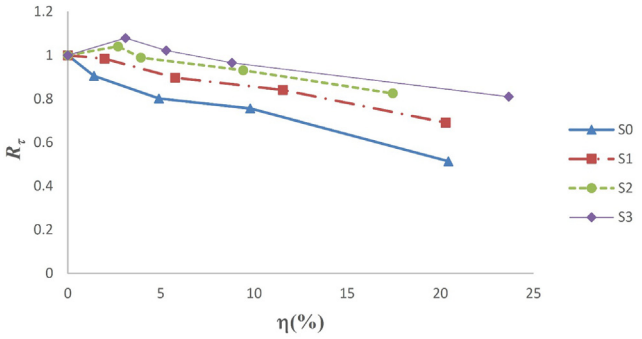

Fig. 10. The relative bond strength-percentage of corrosion.

Table 4
Percentage of increased load, ductility index, and dissipation potential.

	Load (%)	Ductility (%)	Dissipation potential (%)
G1S1C0	11.85	5.57	61.41
G1S1C2	21.63	36.99	172.51
G1S1C5	25.19	−15.77	52.79
G1S1C10	24.51	−11.42	63.38
G1S1C25	50.25	18.71	186.49
G1S2C0	13.83	15.17	94.20
G1S2C2	30.87	64.38	252.69
G1S2C5	40.46	32.78	231.26
G1S2C10	40.36	35.16	233.02
G1S2C25	82.66	61.29	592.91
G1S3C0	17.78	66.87	264.96
G1S3C2	40.37	97.26	651.62
G1S3C5	50.15	32.78	369.63
G1S3C10	50.50	35.16	329.19
G1S3C25	85.50	54.84	502.55

show that an increase in the number of stirrups in the splice region increases the ductility index. To better understand the corrosion effects on the ductility index, the percentage of increase in the ductility index for beams with 1, 2 and 3 stirrups in the splice region (compared to non-stirrup case with corresponding corrosion) is presented in Table 4; as shown, increased ductility index due to the increased stirrups for 2 and 25% corrosion is more compared with other corrosion percentages, and percentage of increase in the ductility index in these two cases is higher than that of the non-corroded case. This means that the stirrup effect on the increased ductility index is more evident in both low and high corrosion cases.

Energy dissipation, the area under the load-displacement curve, is an important factor in studying the structure seismic behavior. The higher the energy dissipation is, the better the specimen will perform (Table 3). As shown, in all cases (0, 1, 2 and 3 stirrups in the splice region), corrosion reduces the energy dissipation potential. However, an increase in the number of stirrups in the splice region, will lead to increases the energy dissipation potential. Table 4 shows the percentage of increase in the energy dissipation potential due to the increase in stirrups in the splice region compared to the non-stirrup case in the corresponding percent corrosion. As shown, the effect of stirrups on increasing the energy dissipation potential in specimens having corroded bars are higher than those lacking them. As with the ductility index in the corroded specimens, the stirrup effect to increase the energy dissipation potential is more in specimens with 2 and 25% corrosion. This means the effects of the increased stirrups in the splice region to increase the energy dissipation potential is more in specimens with low and high corrosion.

4. Conclusions

A review of the experimental studies that have investigated the effects of corrosion on the bond strength reveals that the Pullout Test, the Tension Stiffening Test, and the Actual Beam Test are used to determine such effects. Studies that have used lap-spliced beams for this purpose are quite limited, and the one carried out by Shihata [27] does not consider the effects of the number of stirrups in the splice region. The present work studies the effects of the stirrup spacing on the bond strength of lap-spliced beams having corroded tensile bars in the spliced region. Results of studying and analyzing 20 RC beams having corroded spliced bars with 4 different types of transverse reinforcement in the splice region are as follows:

1- An increase in the number of stirrups in the splice region will increase the bond strength of the corroded/uncorroded lap-spliced beams, but stirrup effects are more obvious in corroded bars. At 25% corrosion, stirrups have the highest effect on the increased bond strength. Under this circumstance, the percentage of bond strength increase for

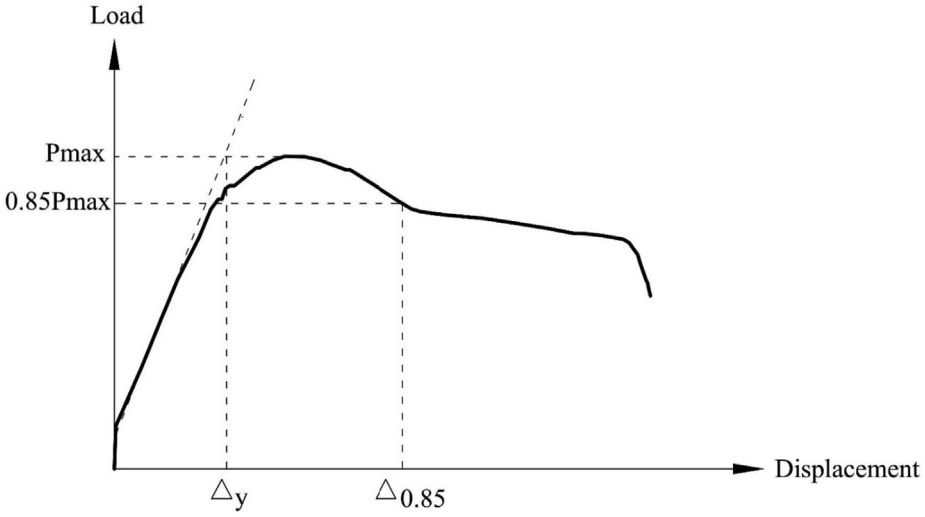

Fig. 11. Calculation method of ductility index [34].

beams with 1, 2, and 3 stirrups in the splice region is 4.24, 5.97, and 4.81 times that in the non-corroded case, respectively.

2- The gradient of the relative bond strength-percentage of corrosion curve in the descending branch is less for specimens with more stirrups; this gradient for beams with 0, 1, 2, and 3 stirrups in the splice region is −0.0198, −0.0154, −0.0136 and −0.0123, respectively.

3- Results show that the beam ductility and energy dissipation potential are affected by the number of stirrups in the splice region; increased number of stirrups increase the energy dissipation potential of the corroded and non-corroded beams. Effects of increased number of stirrups on the increased energy dissipation potential and ductility in specimens with 2 and 25% corrosion (low and high corrosion) are higher.

Declaration of Competing Interest

The authors declare no conflict of interest.

References

[1] H.S. Lee, T. Noguchi, F. Tomosawa, Evaluation of the bond properties between concrete and reinforcement as a function of the degree of reinforcement corrosion, Cem. Concr. Res. 32 (8) (2002) 1313–1318.
[2] K. Lundgren, Modelling the effect of corrosion on bond in reinforced concrete, Mag. Concr. Res. 54 (3) (2002) 165–173.
[3] K. Lundgren, Bond between ribbed bars and concrete. Part 2: the effect of corrosion, Mag. Concr. Res. 57 (7) (2005) 383–395.
[4] J. Cairns, Y. Du, D. Law, Residual bond strength of corroded plain round bars, Mag. Concr. Res. 58 (4) (2006) 221–231.
[5] X.G. Wang, W.P. Zhang, W. Cui, F.H. Wittmann, Bond strength of corroded steel bars in reinforced concrete structural elements strengthened with CFRP sheets, Cem. Concr. Compos. 33 (4) (2011) 513–519.
[6] H. Lin, Y. Zhao, Effects of confinements on the bond strength between concrete and corroded steel bars, Constr. Build. Mater. 118 (2016) 127–138.
[7] J.K. Wight, J.G., Reinforced Concrete Mechanics and Design, sixth ed., Pearson Education, Inc., Upper Saddle River, New Jersey, 2012.
[8] Y. Zhao, H. Lin, K. Wu, W. Jin, Bond behaviour of normal/recycled concrete and corroded steel bars, Constr. Build. Mater. 48 (2013) 348–359.
[9] G.J. Al Sulaimani, M. Kaleemullah, I.A. Basunbul, Rasheeduzzafar, Influence of corrosion and cracking on bond behavior and strength of reinforced concrete members, ACI Struct. J. 87 (2) (1990) 220–231.
[10] M.A. Shayanfar, M. Ghalenovi, Corrosion effects on tension stiffening behavior reinforced concrete, Comput. Concr. 4 (5) (2007) 403–424.
[11] M.W. Law, D. Tang, T.K.C. Molyneaux, R. Gravina, Impact of crack width on bond: confined and unconfined rebar, Mater. Struct. 44 (7) (2011) 1287–1296.
[12] F. Tondolo, Bond behaviour with reinforcement corrosion, Constr. Build. Mater. 93 (2015) 926–932.
[13] X. Zhang, X. Liang, Z. Wang, H. Huang, H. Zhou, An experimental study on effect of steel corrosion on the bond–slip performance of reinforced concrete, in: 5th International Conference on Durability of Concrete Structures, 2016.
[14] H. Yalciner, O. Eren, S. Sensoy, An experimental study on the bond strength between reinforcement bars and concrete as a function of concrete cover, strength and corrosion level, Cem. Concr. Res. 42 (5) (2012) 643–655.
[15] W.P. Zhang, H. Chen, X.L. Gu, Bond behaviour between corroded steel bars and concrete under different strain rates, Mag. Concr. Res. 68 (7) (2016) 364–378.
[16] Y. Ma, Z. Guo, L. Wang, J. Zhang, Experimental investigation of corrosion effect on bond behavior between reinforcing bar and concrete, Constr. Build. Mater. 152 (2017) 240–249.
[17] fib Bulletin 55, Model Code 2010. First complete draft, federation internationale du beton, 292pp, 2010.
[18] J. Rodriguez, L.M. Ortega, J. Casal, Corrosion of reinforcing bars and service life of reinforced concrete structures: corrosion and bond deterioration, in: International conference on concrete across borders, Odense, 1994, pp. 315–326.
[19] C. Fang, K. Lundgren, L. Chen, C. Zhu, Corrosion influence on bond in reinforced concrete, Cem. Concr. Res. 34 (11) (2004) 2159–2167.
[20] B. Sanz, J. Planas, J.M. Sancho, Study of the loss of bond in reinforced concrete specimens with accelerated corrosion by means of push-out tests, Constr. Build. Mater. 160 (2018) 598–609.
[21] L. Amleh, S. Mirza, Corrosion influence on bond between steel and concrete, ACI Struct. J. 96 (3) (1999) 415–423.
[22] J. Dai, E. Kato, M. Iwanami, Yokota, Cracking and tension stiffening behavior of corroded RC members, Report of the port and airport research institute, vol. 46, No. 2, 2007, pp. 1–24.
[23] A. Aryanto, Y. Shinohara, Bond behavior between steel and concrete in low level corrosion of reinforcing steel, 15 WCEE, 2012.
[24] H.R. Kim, W.C. Choi, S.C. Yoon, T. Noguchi, Evaluation of bond properties of reinforced concrete with corroded reinforcement by uniaxial tension testing, Int. J. Concr. Struct. Mater. 10 (3) (2016) 43–52.
[25] P.S. Mangat, M.S. Elgarf, Bond characteristics of corroding reinforcement in concrete beams, Mater. Struct. 32 (216) (1999) 89–97.
[26] R. Al-Hammoud, K. Soudki, T. Topper, Bond analysis of corroded reinforced concrete beams under monotonic and fatigue loads, Cem. Concr. Compos. 32 (3) (2010) 194–203.
[27] Shihata, A., CFRP strengthening of RC beam with corroded lap spliced steel bars, Master of Applied Science Thesis, University of Waterloo, Waterloo, Canada, 2011.
[28] ACI 318R-05, Building code requirements for structural concrete, American Concrete Institute COMMITTEE 318, Farmington Hills, 2011.
[29] DIN EN 10002, Tensile Testing of Metallic Materials- Part 1: Method of Test at Ambient Temperature, DIN- Adopted European Standard, 1991.
[30] T. El Maaddawy, K. Soudki, Effectiveness of impressed current technique to simulate corrosion of steel reinforcement in concrete, ASCE, J. Mater. Civil Eng. 15 (1) (2003) 41–47.
[31] M. Saifullah, L.A. Clark, Effect of corrosion rate on the bond strength of corroded reinforcement, in: R.N. Swamy (Ed.), Corrosion and Corrosion Protections of Steel in Concrete, Sheffield Academic Press, Sheffield, 1994, pp. 591–602.
[32] ASTM standard G1-03, standard practice for preparing, cleaning, and evaluating corrosion test specimens, Annual Book of ASTM Standards, 2003, pp. 17–25.
[33] M.Z. Cohn, M. Barlett, Computer-simulated flexural tests of partially prestressed concrete section, ASCE, J. Struct. Div. 108 (12) (1982) 2747–2765.
[34] M. Rakhshanimehr, M.R. Esfahani, M.R. Kianoush, A. Mohammadzadeh, S.R. Mousavi, Flexural ductility of reinforced concrete beams with lap-spliced bars, Can. J. Civ. Eng. 41 (7) (2014) 594–604.